Photoionized plasmas at Z relevant for astrophysics

R.C. Mancini
Physics Department, University of Nevada, Reno, NV 89557

Science with High-Power Lasers and Pulsed Power Workshop, July 28-30, 2009, Santa Fe, New Mexico

Collaborators

- I. Hall (post-doc.), T. Durmaz (grad. student), UNR

- J.E. Bailey, G. Rochau, T. Nash, SNL
- D. Cohen, Swarthmore College
- M.E. Sherrill, J. Abdallah, LANL
- I.E. Golovkin, J.J. Macfarlane, Prism Computational Sciences
- M.E. Foord, R.F. Heeter, S. Glenzer, LLNL

Photoionized plasmas in the laboratory

- Most of the atomic and radiation physics research that has been done on laboratory plasmas is for collisional plasmas; relatively little work has been performed on laboratory photoionized plasmas.

- Unlike collisional plasmas, the atomic kinetics of photoionized plasmas is driven primarily by a flux of x-ray photons through photoionization and photoexcitation.

- The dearth of laboratory photoionized plasma data is due to inadequate x-ray radiation source energy.

- Z-produced x-rays: E ~ 1 - 2 MJ, fwhm ~ 6 ns, peak power ~ 200 TW.

- Initial experiments done at Z using gas cell and expanding foil type of targets have shown the feasibility of performing and diagnosing laboratory photoionized plasmas*.

- Science opportunity: combined experimental and theory/modeling effort to produce and study well characterized laboratory photoionized plasmas with emphasis on their atomic kinetics and radiative properties.

* J.E. Bailey et al, JQSRT **71**, 157 (2001); R.F. Heeter et al, RSI **72**, 1224 (2001); M.E. Foord et al PRL **93**, 055002 (2004)

Photoionized plasmas in astrophysics

- The availability of high-resolution x-ray spectra recorded by Chandra and XMM-Newton has motivated a renewed effort on the interpretation of x-ray emission from photoionized plasmas, which exist in a large class of astrophysical objects including x-ray binaries and active galactic nuclei.

- Ionization distribution is determined by a balance between photoionization and radiative and dielectronic recombination (PIE).

- Ionization parameter $\xi = 4\pi I/N$, values up to a few thousands erg · cm / s.*

- Artist's illustration of binary system GRO J1655-40: 11,000 light-years away in constellation scorpius.

- Chandra x-ray spectrum data in the 6A to 7A wavelength range shows absorption features in highly-charged ions.

- Detailed analysis of spectrum yields information on accretion disk dynamics.

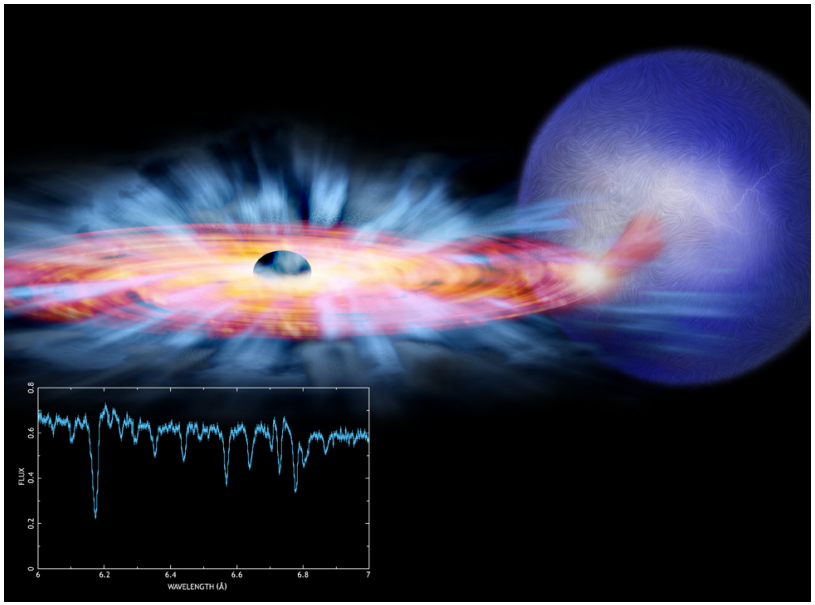

NASA Website

*B.A. Remmington, R.P. Drake and D.D. Ryutov, Rev. Mod. Phys. **78**, 755 (2006)

Some issues with astrophysical plasmas analysis

- Astrophysical plasmas are multi-element (mixture) plasmas, so line identification can be difficult.
- Line absorption spectrum from active galactic nuclei NGC 3783 displays line transitions that have been interpreted as due to line absorption in O, C, N, Fe, Ne, Mg, Si, Ca, … ions.*
- Overlapping and blending of spectral features (lines and edges) makes extraction of column (areal) density (ρR) of individual ions unreliable.
- Line re-interpretation issues, e.g. NGC 3783, λ=21.6 Å, O VII ➔ Ca XVI.*
- In absorption spectra observations, no independent determination of continuum level, i.e. zero level of absorption.
- Plasma modeling and analysis require the assumption of several regions characteristic of different ionization parameters.

*Y. Krongold, F. Nicastro, N.S. Brickhouse, M. Elvis, D.A. Liedahl and S. Mathur, Astrophys. J. **597**, 832 (2003)

Laboratory experiments help in several ways*

- Spectroscopy of single-element, photoionized laboratory plasmas can resolve problems with line identification and interpretation in astrophysical plasmas.
- Well characterized/diagnosed laboratory experiments and detailed modeling are important to study the atomic kinetics, radiation transport and spectroscopy of photoionized plasmas.
- Spectroscopic observations are critical for the understanding of astrophysical photoionized plasmas.
- Some parameters are similar (ξ, Te, Tc, Tb, ρR), but others not (density, size).
- There are several questions to address:
- Investigate and develop benchmarks for photoionized plasmas.
- Steady-state vs. time-dependent?
- Transition from collisional to photoionized plasma?

*R.C. Mancini, J.E. Bailey, J.F. Hawley, T. Kallman, M. Witthoeft, S.J. Rose and H. Takabe, Phys. Plasmas **16**, 041001 (2009)

Laboratory experiments on photoionized plasmas benefit from:

- Previous (extensive) work on detailed theoretical and modeling work on atomic kinetics and radiation physics of collisional plasmas.

- Recent absolute photoionization cross section measurements at the Advanced Light Source (ALS) in Berkeley (R. Phaneuf and collaborators, UNR).

- Experience and developments on plasma spectroscopy diagnostics and instrumentation, e.g. space- and time-resolved crystal spectrometers.

- And laser-driven diagnostics, e.g. interferometry and Thomson scattering.

- **But photoionized plasmas have their own characteristics**:

- different line intensity distributions compared to those of coronal ionization equilibrium,
- plasma is “over-ionized”,
- radiative recombination (RRC) edges with steep drops above threshold.

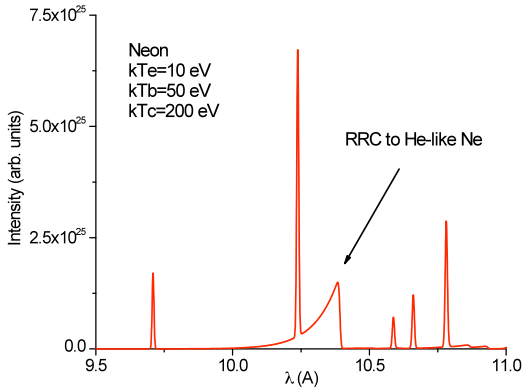

Progression of ξ in Z photoionized plasma experiments is impressive:

- Side gas cell[1]: $\xi = 5 - 7$ erg · cm / s
- Expanding foil[2]: $\xi = 20 - 25$ erg · cm / s
- Top gas cell[3]: $\xi = 100 - 600$ erg · cm / s

Large values of ξ help us achieve two goals:

- investigate new and challenging laboratory plasmas
- increase relevance of laboratory plasma for astrophysics

[1]J.E. Bailey et al, J. Quant. Spectrosc. Radiative Transfer **71**, 157 (2001), and current experiments
[2]M.E. Foord et al, Phys. Rev. Letters **93**, 055002 (2004)
[3]New design for future experiments

Current/future experiments at Z combine previous and new neon gas cell designs, and better diagnostics

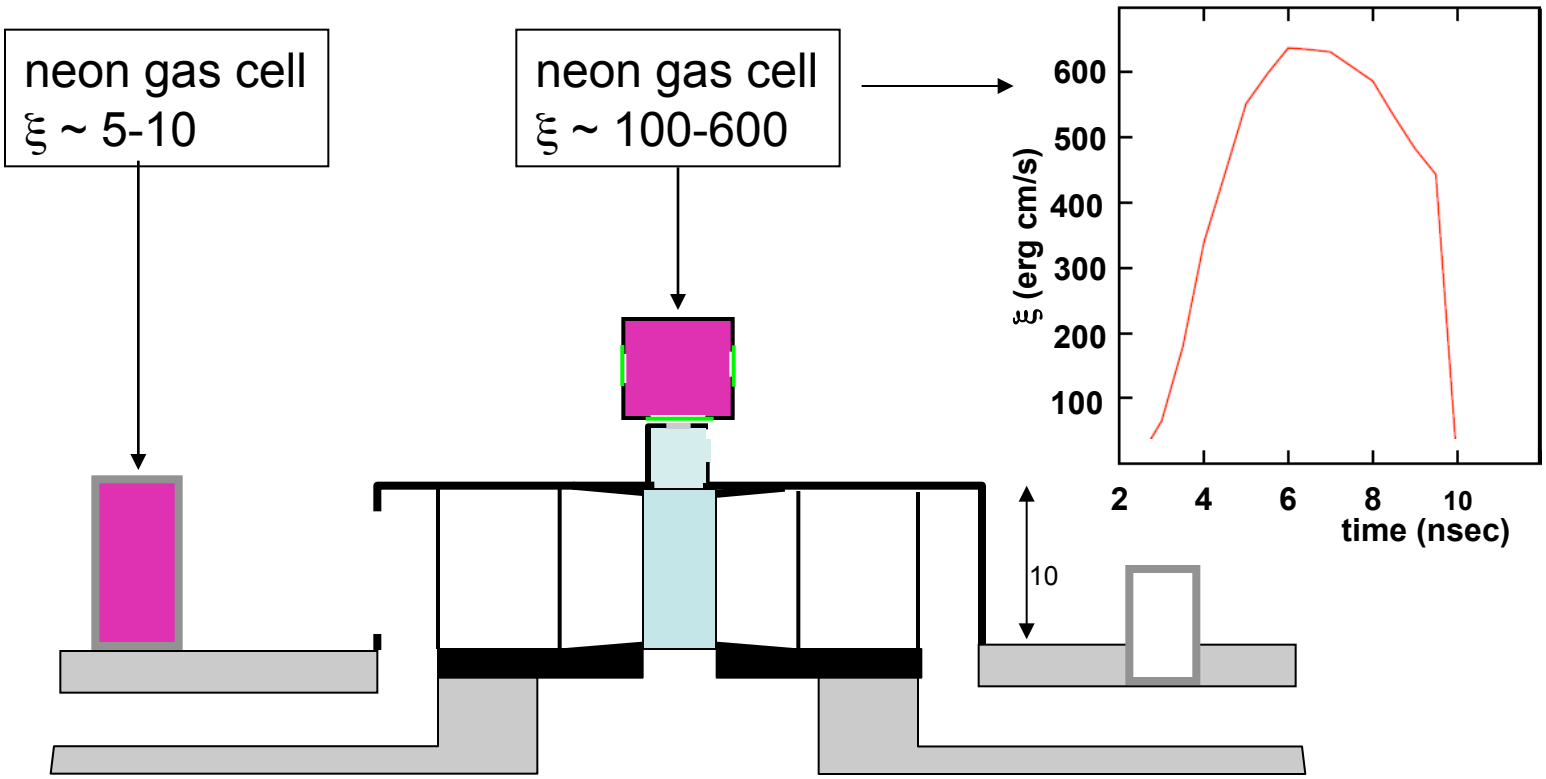

Diagnostics:

Emission spectroscopy – test line ratio and width signatures used by astronomers

Absorption spectroscopy – measure charge state distribution and compare models

Thomson scattering – independent temperature diagnostic

Laser interferometry – plasma density uniformity

View factor calculations model radiation flux at gas cell*

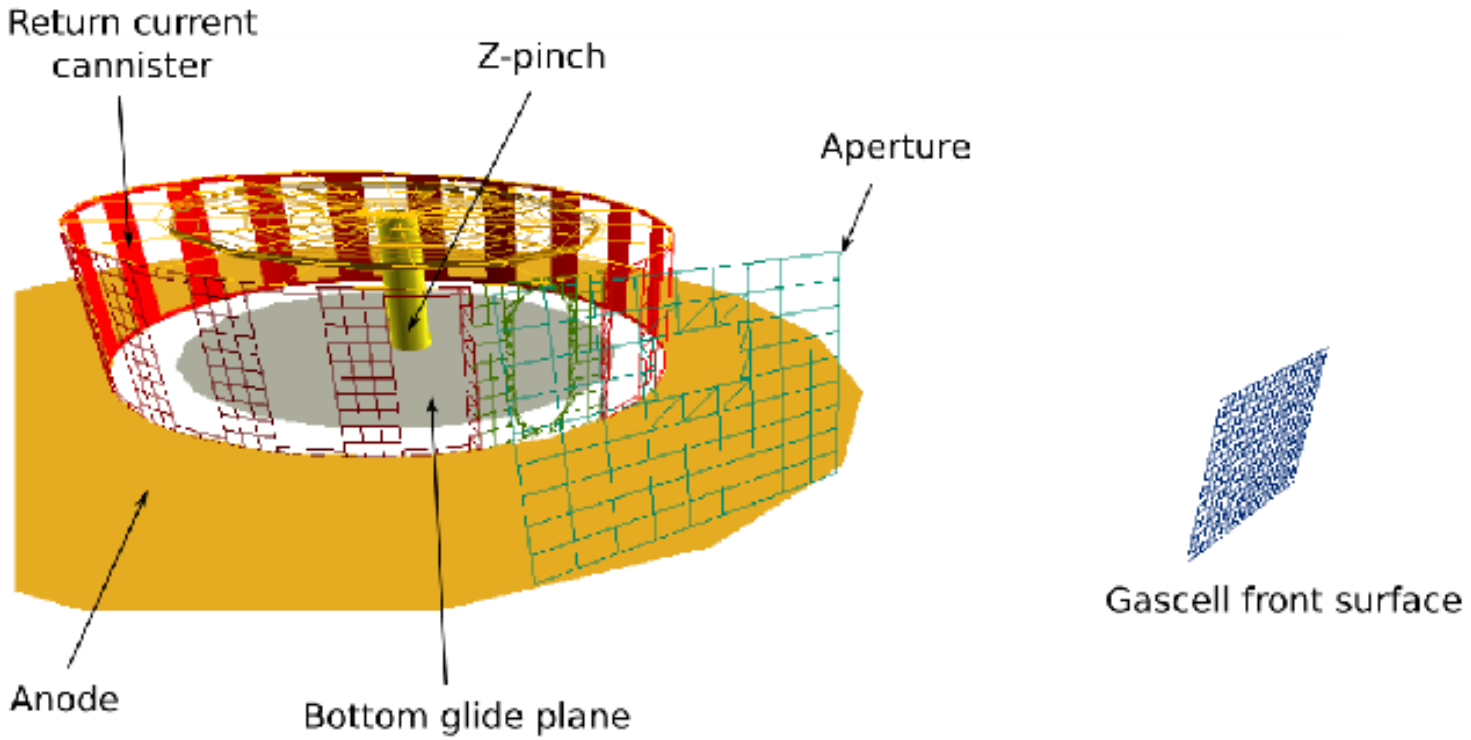

- 2.5cm high return current cannister with 18 slots.
- Gascell front surface at 6.5-7.5cm from Z-pinch axis, at 12^0 above horizontal plane.
- Aperture in place between gascell and Z-pinch to shield gascell from re-emitted X-rays.

- Material Albedos of 0.5-0.85.
- X-ray conversion efficiencies of 0.6.
- Z-pinch radius and power time dependence from Z shot #z541.

*J. MacFarlane, J. Quant. Spectrosc. Radiative Transfer **81**, 287 (2003)

X-ray flux distribution at the gas cell*

The radiation field at the gascell front surface is *non-Planckian* due to geometrical dilution of Z-pinch emission and contribution of re-emitted radiation.

Radiation field at centre of gascell front surface (at peak Z-pinch emission)

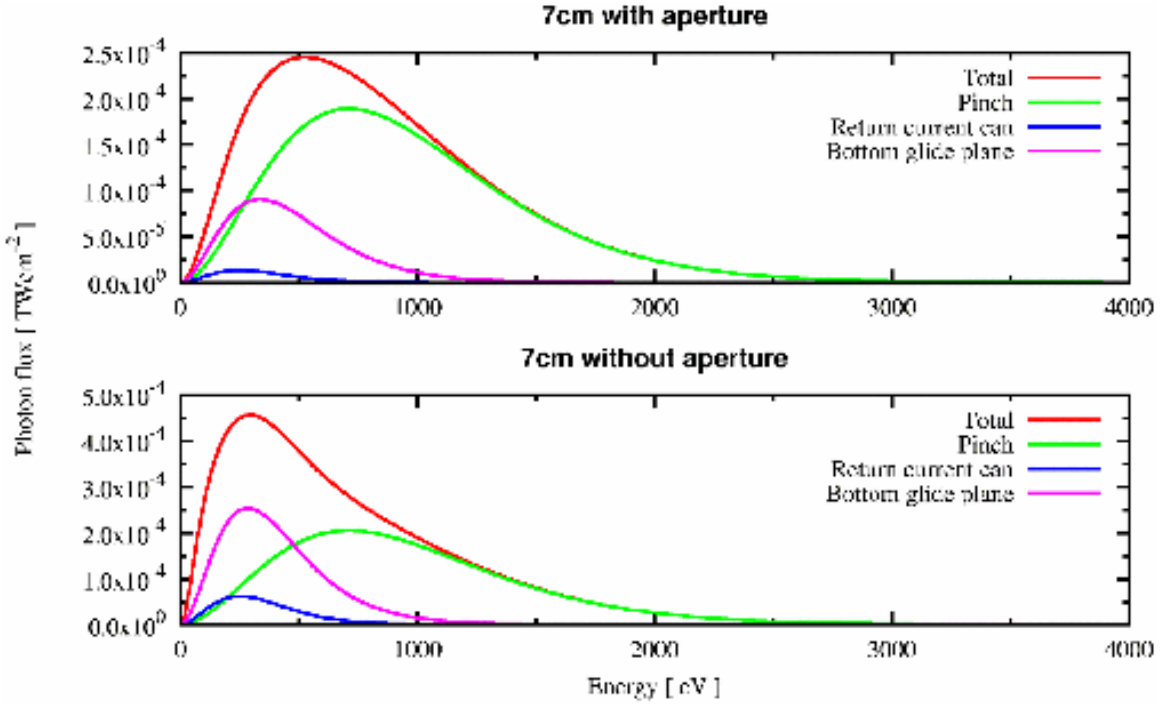

- Aperture reduces contributions to total flux from return current can and bottom glide plane.

*I. Hall et al, Astrophysics and Space Science (2008)

Neon atomic kinetics: atomic processes

Spontaneous Radiative Decay/Photoexcitation	$X^{q+*} \leftrightarrow X^{q+} + h\nu$
Collisional Excitation/Deexcitation	$X^{q+} + e^- \leftrightarrow X^{q+*} + e^-$
Collisional Ionization/Three-body recombination	$X^{q+} + e^- \leftrightarrow X^{(q+1)+} + 2e^-$
Autoionization/Electron Capture	$X^{q+*} \leftrightarrow X^{(q+1)+} + e^-$
Radiative Recombination/Photoionization	$X^{(q+1)+} + e^- \leftrightarrow + X^{q+} h\nu$

External radiation driven processes impact the atomic kinetics of the plasma by driving further photoexcitation and photoionization

Detail of atomic processes

Ion	# of fine struct. energy levels
Ne^{6+}	10
Ne^{7+}	825
Ne^{8+}	125
Ne^{9+}	25

	# of transitions				
Process	**Ne^{6+}**	**Ne^{7+}**	**Ne^{8+}**	**Ne^{9+}**	Total
Rad Decay	*15*	*106,216*	*2,327*	*99*	***108,657***
Autoionization	*-*	*868*	*9*	*-*	***877***
Coll Excitation	*44*	*280,717*	*6,726*	*298*	***287,785***
Coll Ionization	*3,340*	*79,915*	*1,489*	*24*	***84,768***
Rad Recombination	*3,331*	*79,234*	*1,454*	*24*	***84,043***

Atomic rates (s^{-1}): photoionization is dominant (I)

Te = 10 eV **Tb = 50 eV**	Li	He	H
Photo Ioniz.	1.286e+09	1.388e+08	3.621e+07
Rad Rec.	3.976e+06	1.722e+07	4.282e+07
Collis Ioniz.	6.368e-02	2.291e-44	3.429e-52
Three-body rec	1.290e+05	3.622e+03	4.687e+03
Auto Ioniz.	4.118e+13	2.161e+14	-
Electron Capt.	2.012e-19	4.994e-22	-

P_{Ne} = 30 Torr, Na = 1×10^{18} cm^{-3}, Ne = 8×10^{18} cm^{-3}, T_c = 200 eV, L = 1 cm

Atomic rates (s^{-1}): photoionization is dominant (II)

Te = 25 eV **Tb = 30 eV**	Li	He	H
Photo Ioniz.	1.667e+08	1.799e+07	4.693e+06
Rad Rec.	2.565e+06	1.084e+07	2.690e+07
Collis Ioniz.	1.414e+05	3.420e-13	1.483e-16
Three-body rec	4.580e+04	1.097e+03	1.634e+03
Auto Ioniz.	4.118e+13	2.161e+14	-
Electron Capt.	4.764e-03	5.089e-04	-

P_{Ne} = 30 Torr, Na = 1×10^{18} cm^{-3}, Ne = 8×10^{18} cm^{-3}, T_c = 200 eV, L = 1 cm

Transmission spectrum through Ne photoionized plasma

- N_e = 8 x10^{18} cm^{-3}
- T_e = 10 eV
- T_b = 45 eV
- T_c = 200 eV

- Line transitions:
  - $1s^1$ - $2p^1$ (Lyα)
  - $1s^1$ - $3p^1$ (Lyβ)

  - $1s^2$ – $1s^1$ $2p^1$ (Heα)
  - $1s^2$ – $1s^1$ $3p^1$ (Heβ)
  - $1s^2$ – $1s^1$ $4p^1$ (Heγ)
  - $1s^2$ – $1s^1$ $5p^1$ (Heδ)
  - $1s^2$ – $1s^1$ $6p^1$ (Heε)
  - $1s^2$ – $1s^1$ $7p^1$
  - $1s^2$ – $1s^1$ $8p^1$
  - $1s^2$ – $1s^1$ $9p^1$
  - $1s^2$ – $1s^1$ $10p^1$

  - $1s^2$ 2L – $1s^1$ 2L np^1 (n=3-10)

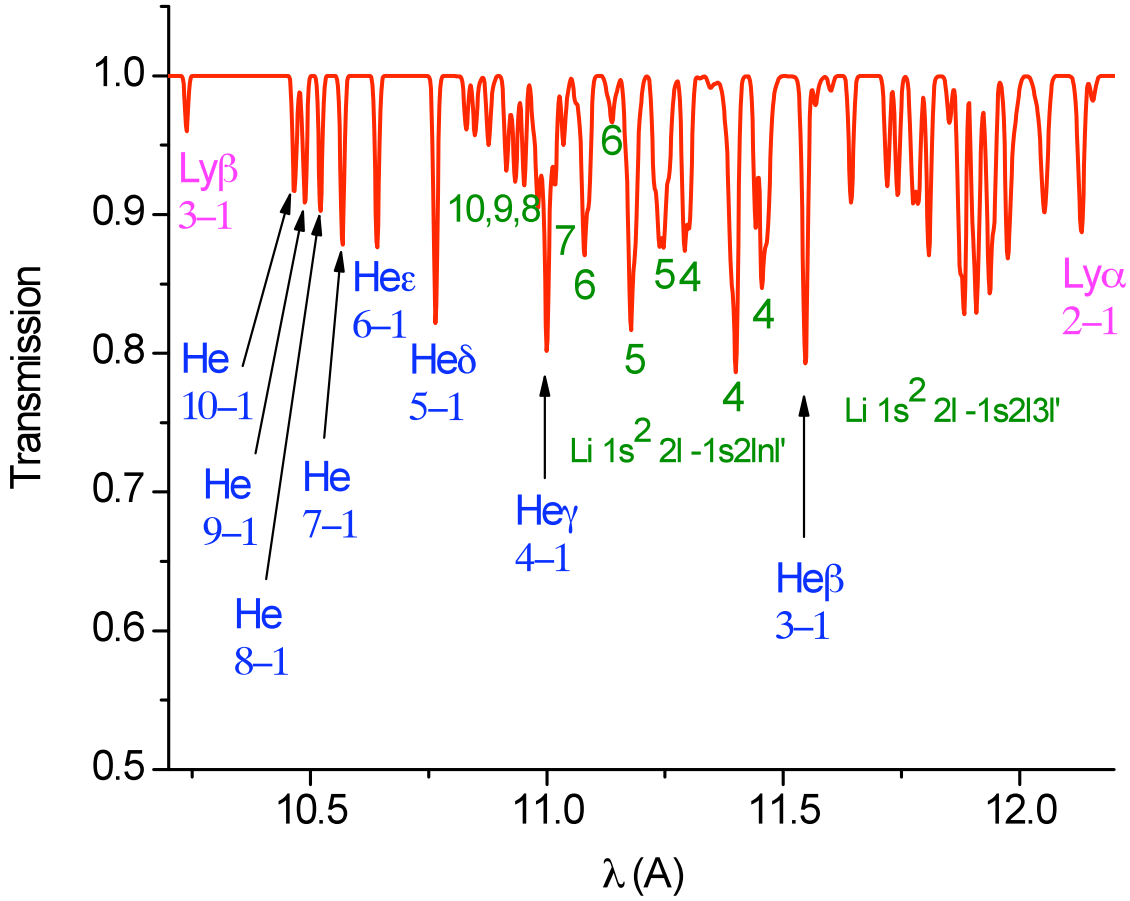

Side, cm-scale gas cells have been fielded at Z

- Photoionized plasma experiments are performed as "ride-along" in Z opacity shots
- Gas cell targets were designed at Sandia and fabricated in the UNR Physics machine shop

Two-window gas cell

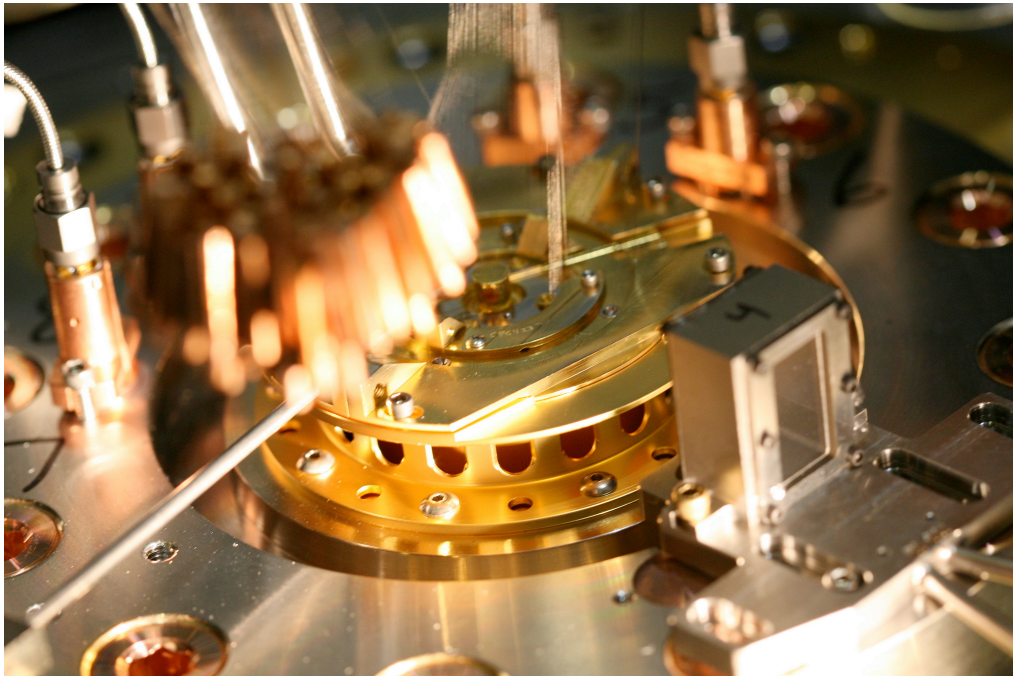

Four-window gas cell

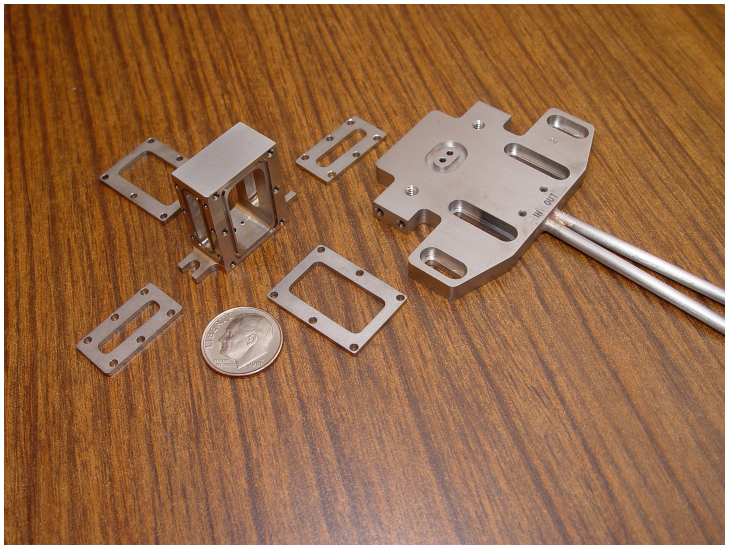

TREX* spectrometers record time-integrated and gated spectra

- Two sets of brass plates, aluminum wedges and steel spoolers were fabricated at the UNR Physics machine shop customized for new KAP crystals

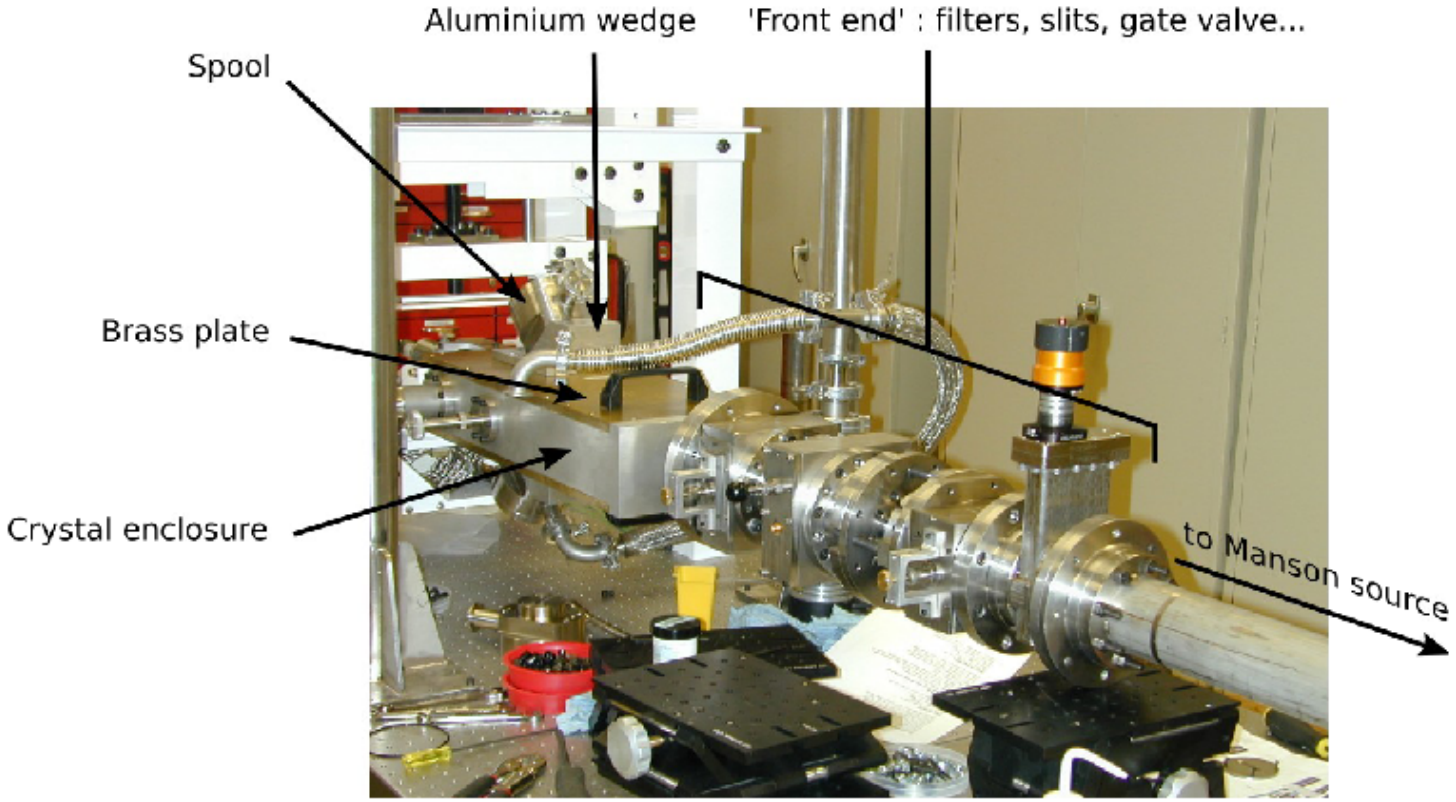

* P.W. Lake, J.E. Bailey et al, Rev. Sci. Instrum. **75**, 3690 (2004); P.W. Lake, J.E. Bailey et al, Rev. Sci. Instrum. **77**, 10F315 (2006)

Data processing: from raw data to transmission

z1894 TREX time-integrated

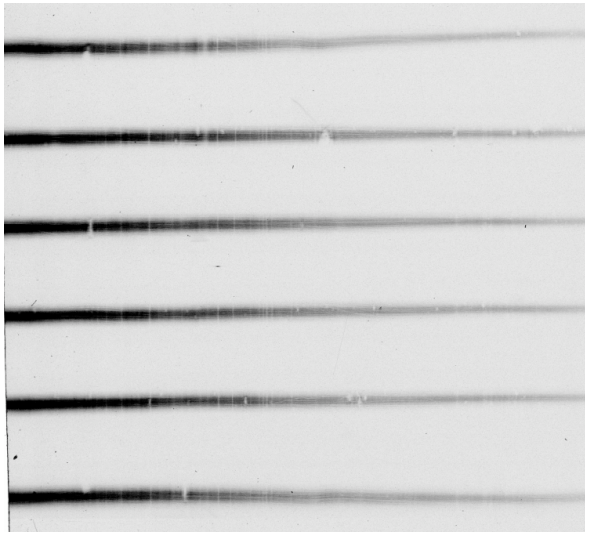

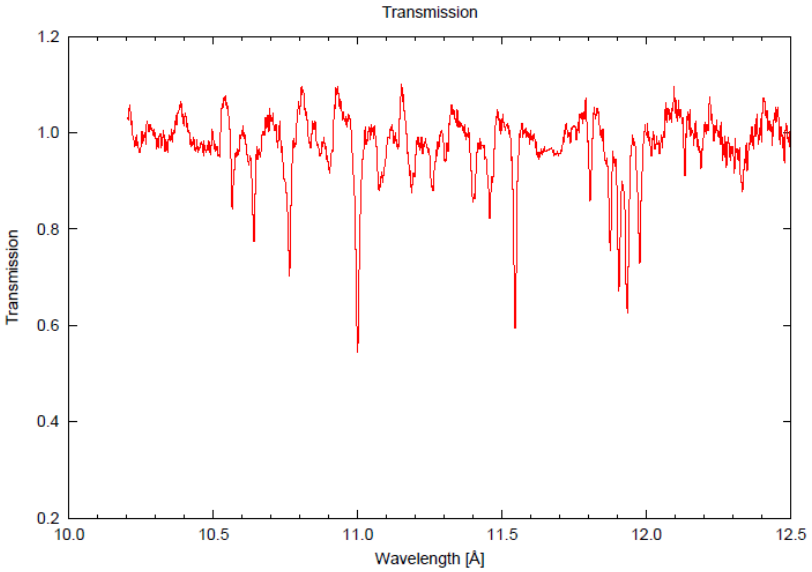

- Remove contribution of 2nd order reflection photons from film density
- Use film calibration to convert from film density to exposure
- Correct for transmission through filters (Be, mylar, Kimfol), and crystal reflectivity
- Determine zero level of absorption for line transmission
- Extract transmission spectrum $e^{-\tau\nu}$

Transmission spectrum shows absorption in three Ne ions

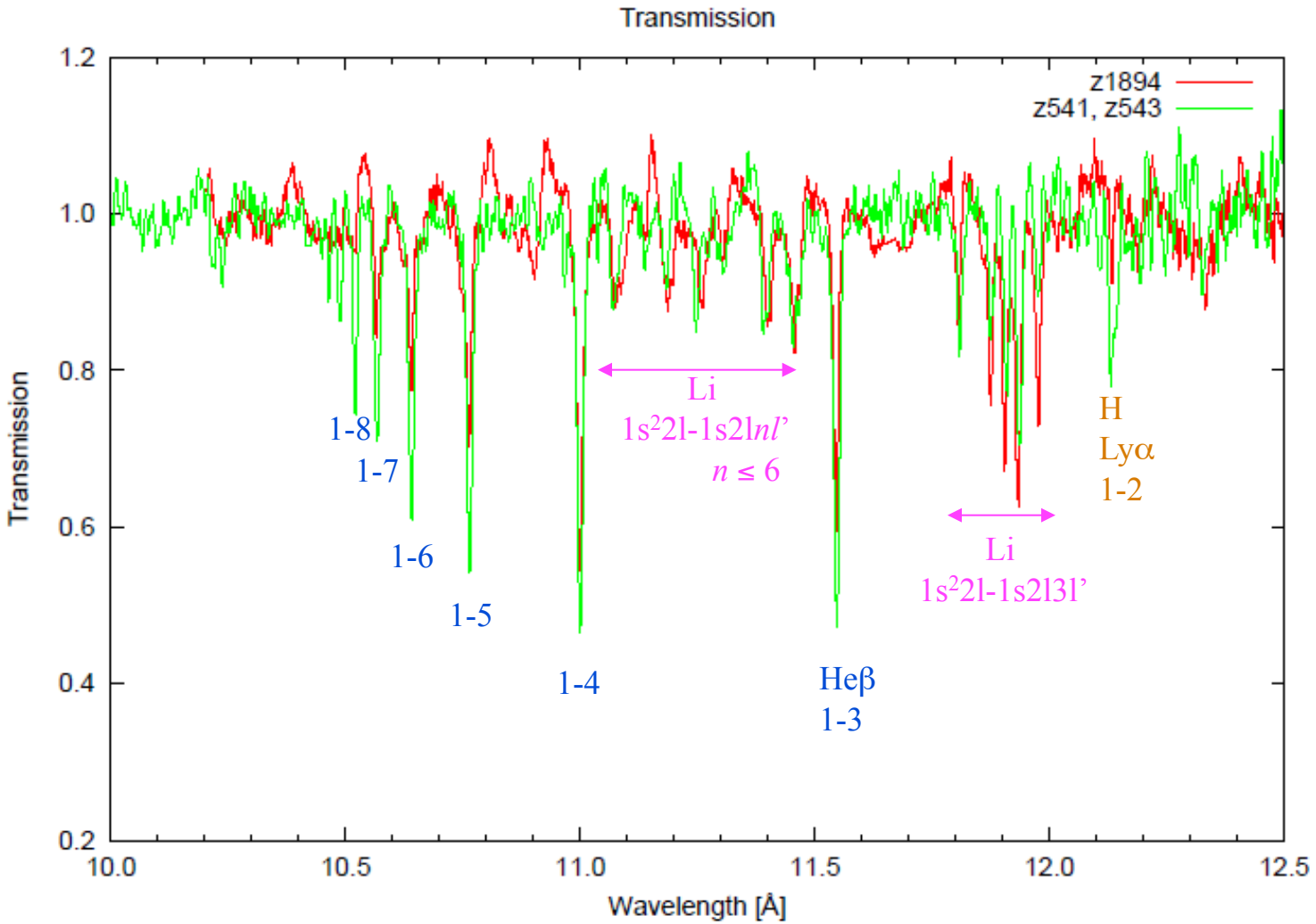

Charge state distribution analysis

- Is it possible to extract information about the charge state distribution without using atomic kinetics calculations?
- Absorption spectra show contributions from line transitions in three ionization stages of Ne: Li-, He- and H-like Ne
- Assume most of the population is in ground and low-excited states of these ionization stages of Ne
- For each ion, calculate the total cross section σ_ν for transitions arising from a given energy level:
  - Li-like Ne: $1s^2$ 2s (1 f. s.) and $1s^2$ 2p (2 f. s.)
  - He-like Ne: $1s^2$ (1 f. s.)
  - H-like Ne: 1s (1 f. s.)

Total cross sections have several contributions

- Total cross sections have contributions from photoexcitation line transitions as well as direct photoionization (thresholds)
- For each ion, calculate the total cross section σ_ν for transitions arising from a given energy level
- Total cross section $\sigma_\nu = \Sigma\, (\pi e^2/mc) \cdot f \cdot \varphi_\nu + \Sigma\, \sigma_\nu\, (dpi)$
- Need atomic structure and scattering data, and line shapes
- Absorption oscillator strengths *f* and direct photoionization cross sections σ_ν (*dpi*) were computed with the HULLAC and Los Alamos atomic structure and scattering codes, and the PRISM suite of codes

Photoexcitation transitions in Li and He-like Ne

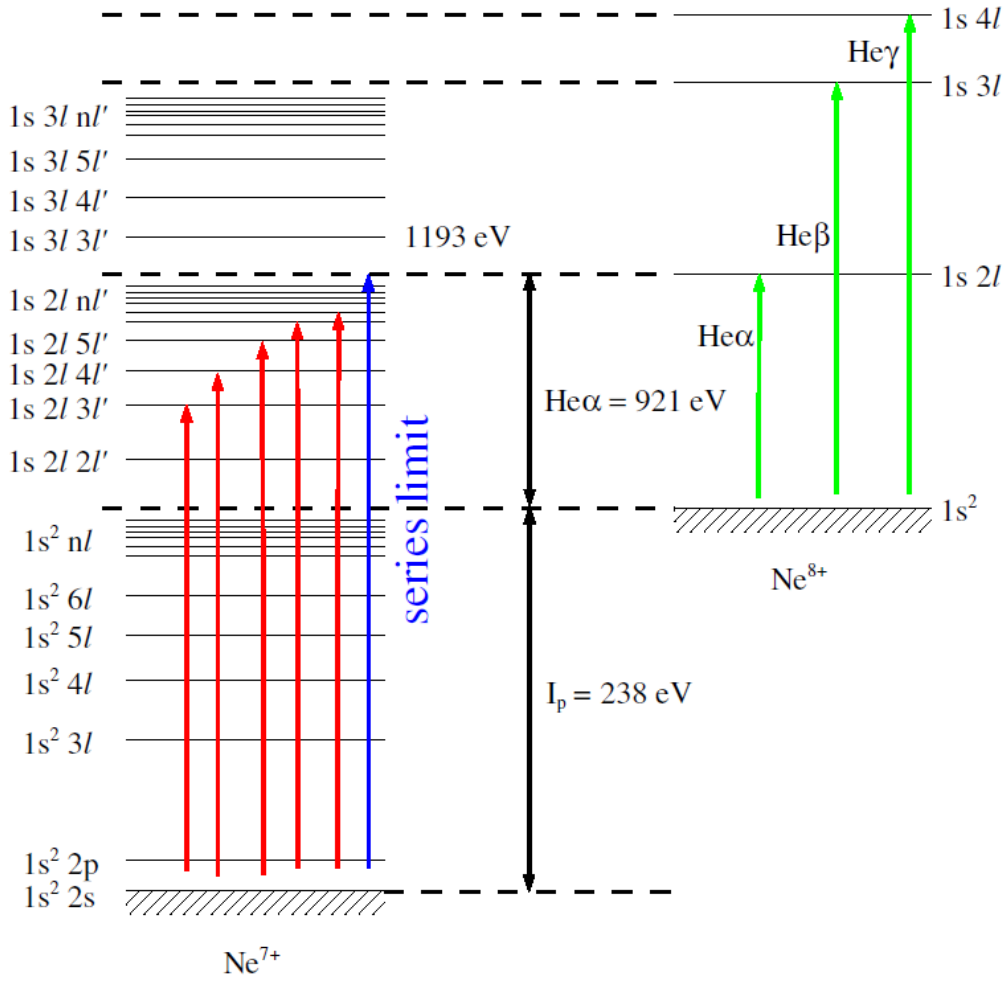

- He-like series:

  Heα $1s^2$ – 1s2p

  Heβ $1s^2$ – 1s3p

  Heγ $1s^2$ – 1s4p

  $1s^2$ – 1snp

- Li-like series:

  $1s^2$ 2l – 1s 2l 2p

  $1s^2$ 2l – 1s 2l 3p

  $1s^2$ 2l – 1s 2l 4p

  $1s^2$ 2l – 1s 2l np

- Li-like series limit: 1159 eV

Total cross sections in Li-like Ne

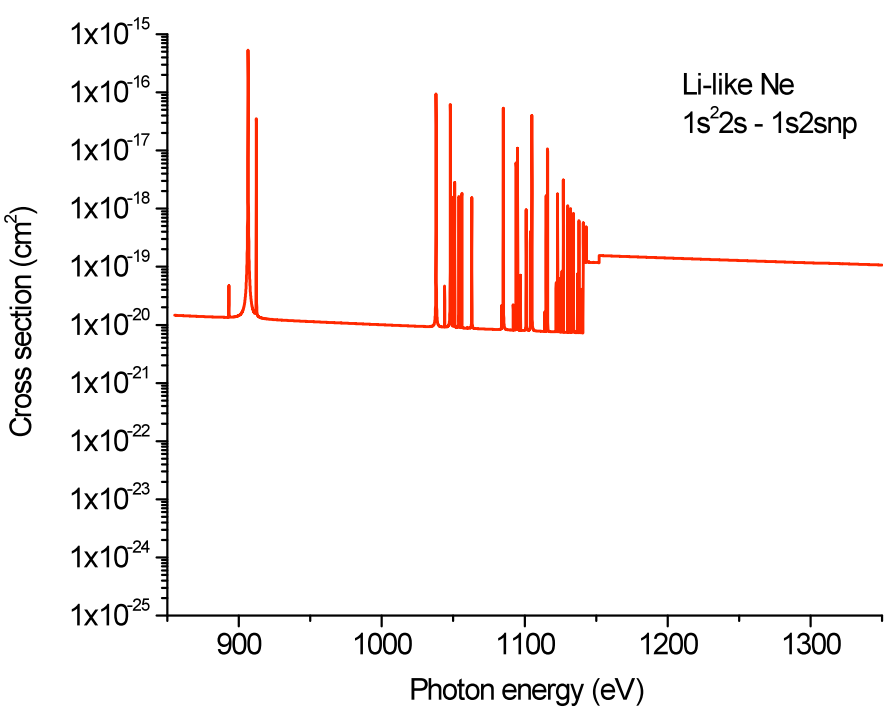

197 line transitions
18 photoionization thresholds

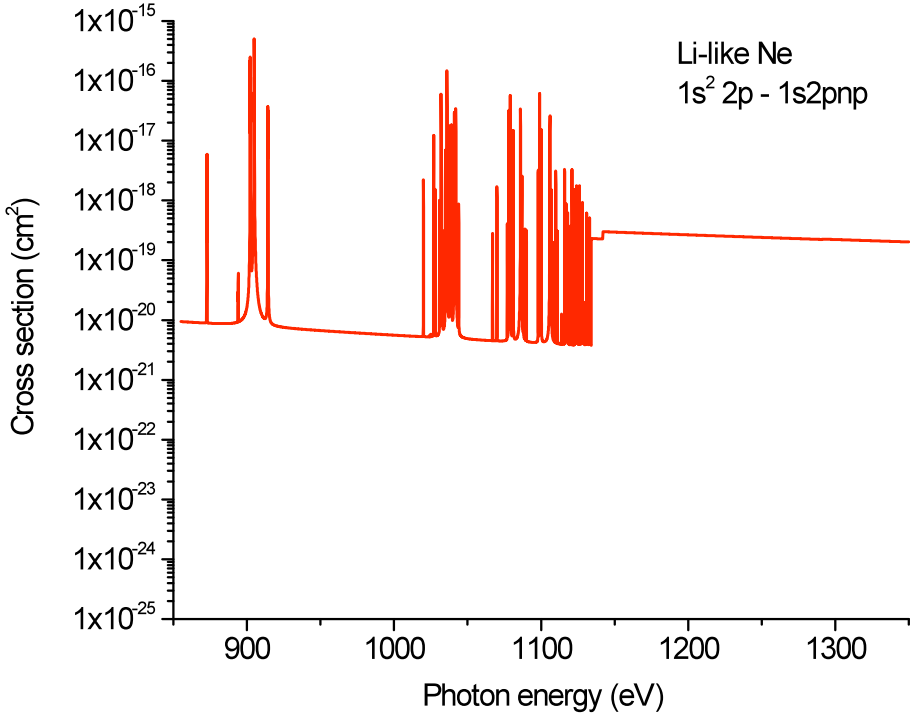

511 line transitions
69 photoionization thresholds

Total cross sections in He- and H-like Ne

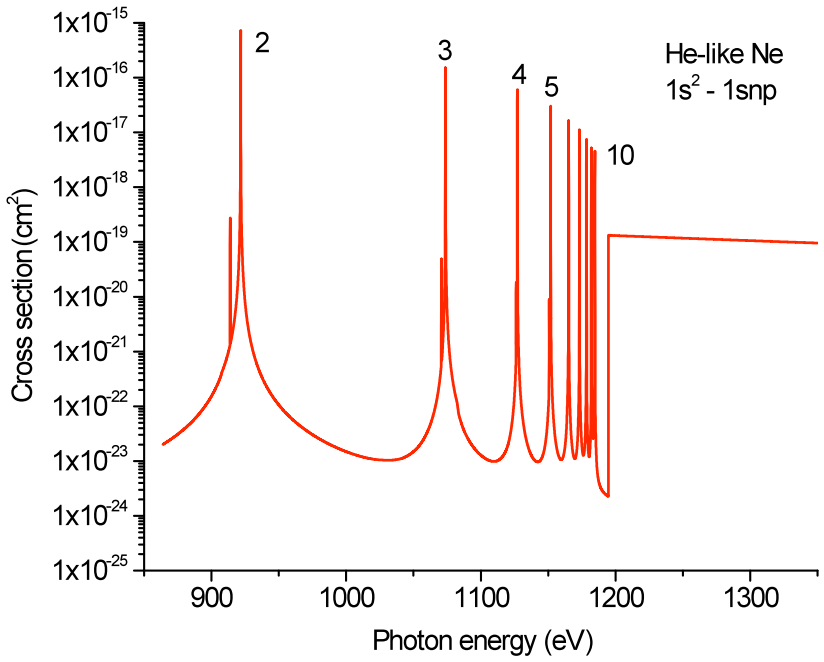

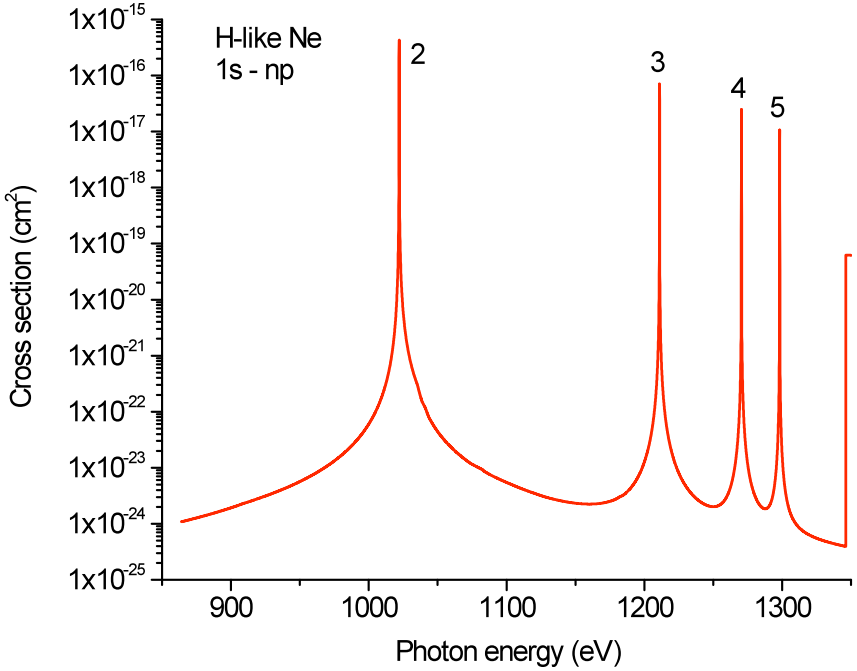

Spectral line shapes

- Spectral line shapes are Voigt profiles that include the effects of natural and Doppler broadening
- However, for high-*n* members of the He-like series of line transitions Stark broadening due to plasma ions and electrons becomes important
- Stark broadening is mainly Ne dependent, and weakly Te dependent
- A series of Stark broadened line shape calculations were done for the He-like lines including the effects of plasma ions and electrons
- Standard Stark-broadening theory approximation: static ions and dynamic electrons[1,2], microfield distribution function computed with the APEX model[3]
- Stark-broadened line shapes also include natural and Doppler broadening

[1]L.A. Woltz et al, Phys. Rev. A **38**, 4766 (1988)
[2]R.C. Mancini et al. Comp. Phys. Comm. **63**, 314 (1991)
[3]C.A. Iglesias et al, Phys. Rev. A **31**, 1698 (1985)

Stark broadening effect can dominate line width

- Full width half maximum of Voigt line profile, natural and Doppler broadening
- Full width half maximum of Stark-broadened He-like neon series line profiles
- Stark width increases with *n*

$N_a = 1\times10^{18}cm^{-3}$

$N_e = 8\times10^{18}cm^{-3}$

$T_e = T_i = 30eV$

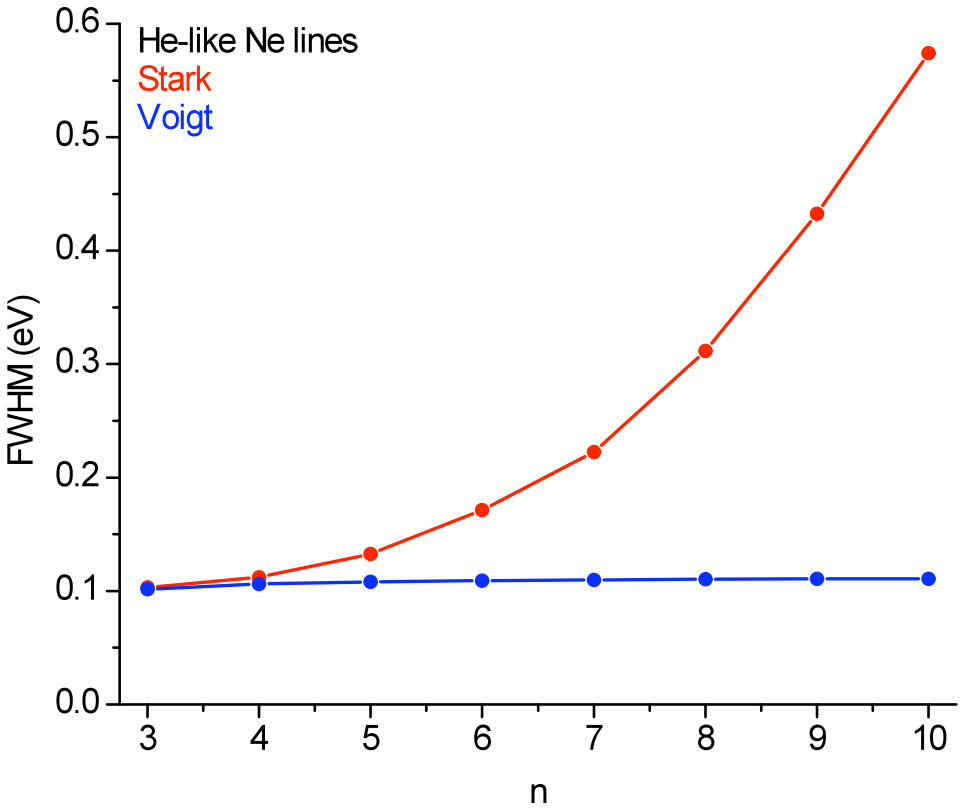

Charge state distribution extraction

- Photon-energy dependent opacity depends on photon-energy dependent cross sections (known) and population number densities (not known)

- Opacity has four contributions:

$$\kappa_\nu = \Sigma\, N\,(\textit{initial state}) \cdot \sigma_\nu\,(\textit{initial state}) = N\,(1s^2\ 2s) \cdot \sigma_\nu\,(1s^2\ 2s) +$$

$$N\,(1s^2\ 2p) \cdot \sigma_\nu\,(1s^2\ 2p) + N\,(1s^2) \cdot \sigma_\nu\,(1s^2) + N\,(1s) \cdot \sigma_\nu\,(1s)$$

- Optical depth $\tau_\nu = \kappa_\nu \cdot L$

- Theoretical transmission $T_\nu = e^{-\tau\nu}$ → convolve with instrum. function

- Search for population number densities that yield the best fit to the experimental photon-energy dependent transmission

- How do we drive the search in parameter space? → Genetic Algorithm

Theoretical fit to the experimental transmission

Population number densities:

$N(1s^2\ 2s) = 3.6 \times 10^{16}\ cm^{-3}$

$N(1s^2\ 2p) = 3.6 \times 10^{16}\ cm^{-3}$

$N(1s^2) = 1.98 \times 10^{18}\ cm^{-3}$

$N(1s) = 1.4 \times 10^{16}\ cm^{-3}$

$Na \approx 2.1 \times 10^{18}\ cm^{-3}$

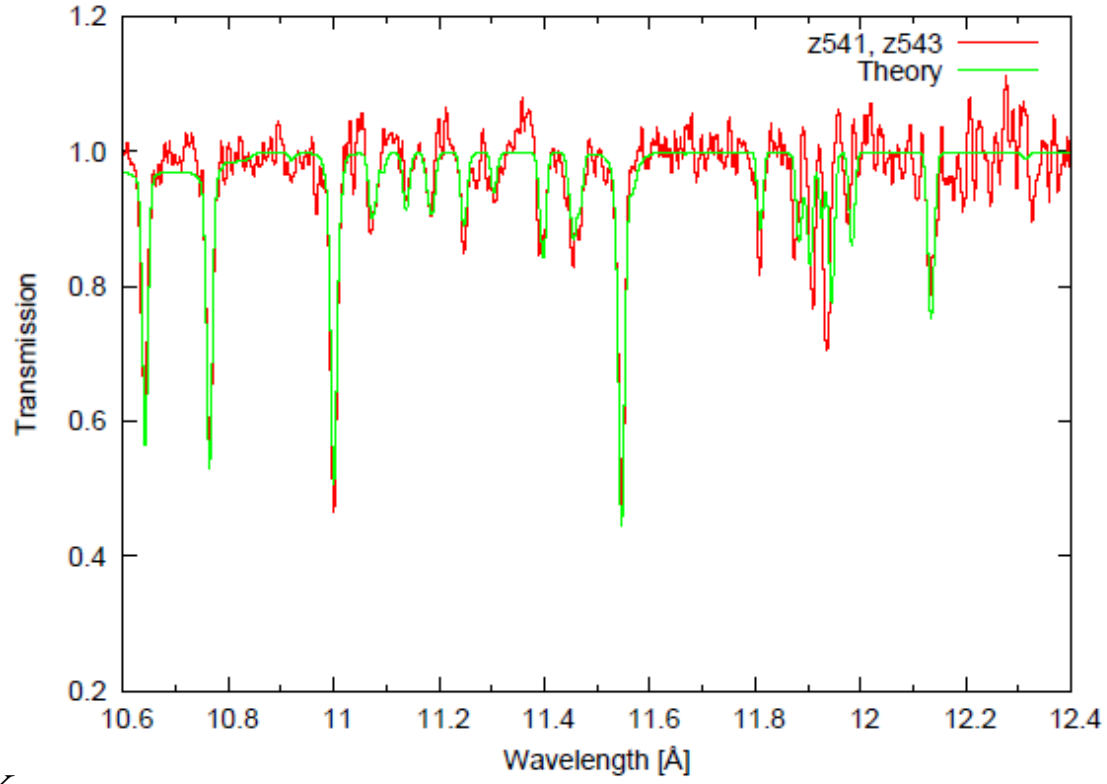

H-like Ne Lyβ (1-3) is very weak

No evidence of line transitions in Be-like Ne

Charge state distribution (CSD) analysis results

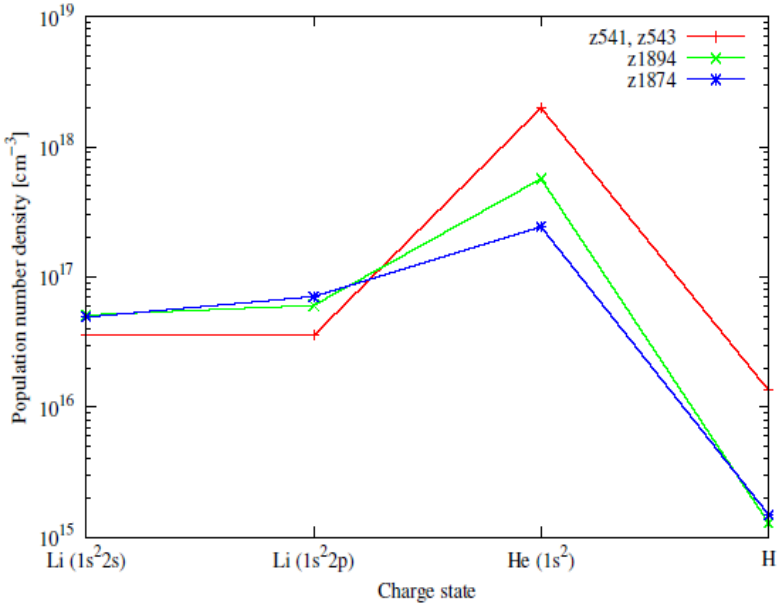

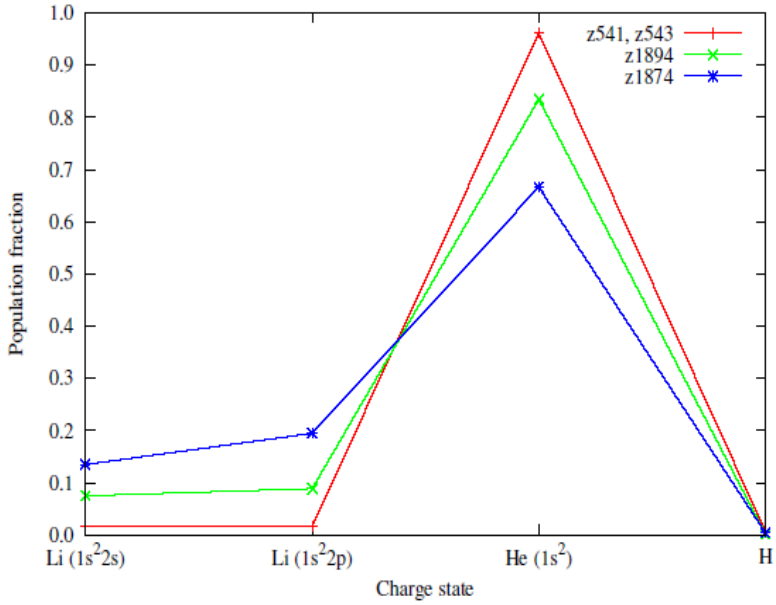

- The application of the CSD method to three Z shots shows the feasibility of this analysis
- In addition: it gives Na which connects to filling pressure conditions P_{Ne}

Summary

- Basic science at Z: combined experimental and theory/modeling effort to produce and study well characterized laboratory photoionized plasmas with emphasis on their atomic kinetics and radiative properties.

- We can do high-energy density laboratory astrophysics while cutting into a new and unexplored laboratory plasma regime.

- Data from large-ξ photoionized plasmas is needed to benchmark and constrain models and codes used in laboratory and astrophysical plasmas.

- This is work in progress …

  - recorded time-integrated transmission spectra,
  - developed new CSD analysis method,
  - gas fill pressure at shot time via target mounted pressure sensor,
  - for current experiments: improve gated measurements,
  - need to do more work on self-emission measurement,
  - for future experiments: re-calculate top gas cell design using recent data from Z dynamic hohlraums,
  - establish laser-driven diagnostics for photoionized plasmas.

This work is supported by DOE Stewardship Science Academic Alliances Grant DE-FG52-06NA27587, and SNL